

Prevalence and characteristics of idiopathic right ventricular outflow tract arrhythmias associated with J-waves

Yoshihiro Yamashina^{1,2}, Tetsuo Yagi^{1*}, Akio Namekawa¹, Akihiko Ishida¹, Hirokazu Sato^{1,2}, Takashi Nakagawa¹, Manjirou Sakuramoto¹, Eiji Sato^{1,2}, and Tomoyuki Yambe²

¹Division of Cardiology, Sendai City Hospital, Wakabayashi-ku, Shimizukouji3-1, Sendai, Japan; and ²Department of Medical Engineering and Cardiology, Institute of Development, Aging and Cancer, Tohoku University, Sendai, Japan

Received 24 May 2011; accepted after revision 6 July 2011; online publish-ahead-of-print 15 August 2011

Aim	The arrhythmogenic relationship between the presence of J-waves during sinus rhythm and idiopathic ventricular tachycardia (VT) or pre-mature ventricular contractions (PVCs) originating from the right ventricular outflow tract (RVOT) has not been reported. The aim of this study was to investigate the prevalence and characteristics of idiopathic RVOT–VT/PVCs associated with J-waves.
Methods and results	The study enrolled 138 consecutive idiopathic RVOT–VT/PVC patients undergoing radiofrequency catheter ablation (RFCA) and 276 age- and gender-matched control subjects. The prevalence of J-waves was assessed in each cohort, and the clinical and electrophysiological data were compared between the RVOT–VT/PVC patients with J-waves (J-RVOT–VT/PVC group) and those without (non-J-RVOT–VT/PVC group). J-waves were more common among patients with idiopathic RVOT–VT/PVCs than among the matched control subjects (40 vs. 16% $P < 0.001$). The J-RVOT–VT/PVC group had a higher incidence of sustained VT (25 vs. 5%, $P < 0.01$), shorter VT cycle length (302 ± 57 vs. 351 ± 58 ms, $P < 0.001$), and more episodes of syncope (25 vs. 2%, $P < 0.001$) than did the non-J-RVOT–VT/PVC group. However, no patients demonstrated any ventricular fibrillation (VF) or cardiac sudden death in either group.
Conclusions	There was a high prevalence of J-waves in the idiopathic RVOT–VT/PVC patients referred for RFCA. Although patients with idiopathic RVOT arrhythmias associated with J-waves might have a more enhanced arrhythmogenicity than those without J-waves, the significance of those J-waves was limited in terms of the prognosis and VF.
Keywords	J-waves • Pre-mature ventricular contraction • Right ventricular outflow tract • Ventricular tachycardia

Introduction

Recently, the presence of J-waves (notching or slurring after the QRS complex during sinus rhythm) in the inferior-lateral leads of the 12-lead electrocardiogram (ECG) has been reported to be associated with ventricular arrhythmias.^{1–8} In the initial case-control study describing an idiopathic ventricular fibrillation (VF) associated with J-waves (J-wave syndrome) published by Haïssaguerre *et al.*¹ when pre-mature ventricular contractions (PVCs) were present and documented in a J-wave syndrome patient, their origin was

from the area of the J-waves and it was considered as a strong argument to link idiopathic VF and J-waves in the inferior-lateral region. To the best of our knowledge the arrhythmogenic relationship between idiopathic ventricular tachycardia (VT)/PVCs arising from the right ventricular outflow tract (RVOT), which are the most common type of ventricular arrhythmias in structurally normal hearts,^{9,10} and J-waves has not been previously reported. However, we actually encountered a case of unexpected sudden death due to VF while observing for J-waves and suspected idiopathic RVOT–PVCs (Figure 1).¹¹ Another case report also described an

* Corresponding author. Tel: +81 022 266 7111; fax: +81 022 211 8972, Email: tetsuo.yagi@nifty.com

Published on behalf of the European Society of Cardiology. All rights reserved. © The Author 2011. For permissions please email: journals.permissions@oup.com.

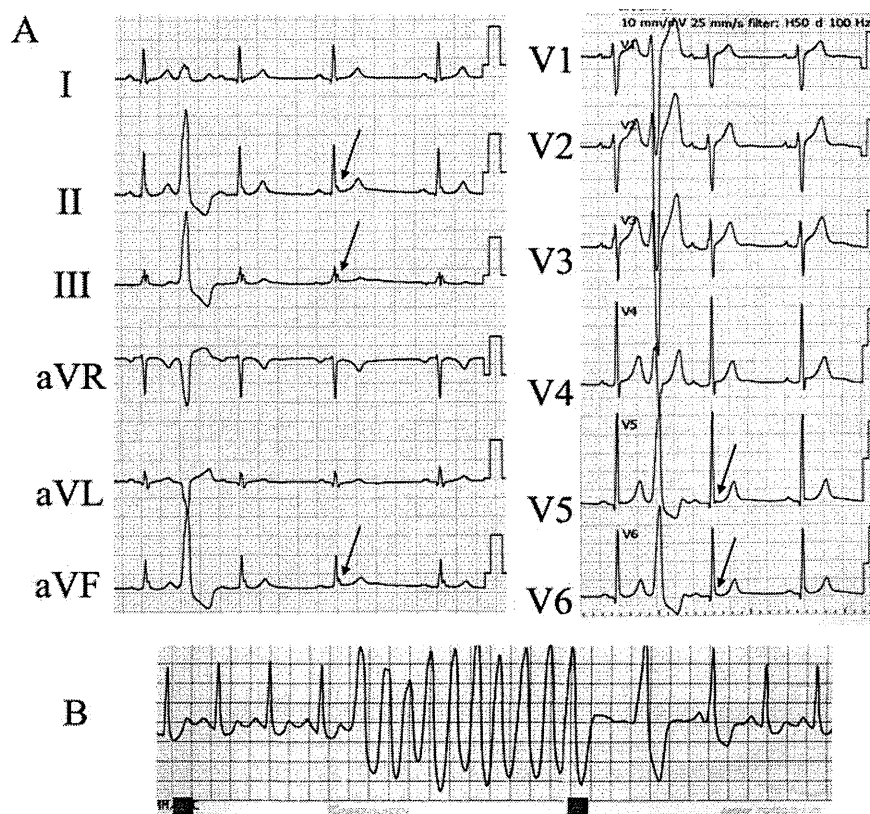


Figure 1 (A) A 12-lead electrocardiogram in a 45-year-old male who suffered from sudden cardiac death due to ventricular fibrillation.¹¹ This electrocardiogram was recorded incidentally 1 month before his sudden death. He had no evidence of any cardiac disease. The electrocardiogram demonstrates J-waves (arrow) in the inferior leads and V5–6 during sinus rhythm and pre-mature ventricular contractions with a left bundle branch block and inferior-axis deviation. (B) The monitored electrocardiogram in the same patient after the resuscitation. A rapid non-sustained ventricular tachycardia was observed (cycle length = 210 ms). Unfortunately, we could not perform an electrophysiological evaluation or radiofrequency catheter ablation for this patient because he died due to hypoxic encephalopathy 5 days after the resuscitation. Adapted with permission from the publisher of the *Journal of Sendai City Hospital* (in Japanese).

exercise-induced sustained RVOT-type VT associated with J point elevation in the inferior leads in a patient without apparent heart disease.¹² It is unknown as to whether or not the presence of J-waves affects the arrhythmogenicity of idiopathic RVOT-VT/PVCs. The purpose of this study was to investigate the prevalence and characteristics of idiopathic RVOT-VT/PVCs associated with J-waves.

Methods

Study population

The study was approved by the institutional review board. We reviewed the database of 138 consecutive patients (mean age 44 ± 15 years, 45 males) in whom radiofrequency catheter ablation (RFCA) was conducted for the treatment of idiopathic RVOT-VT/PVCs at our institute. No patients had any structural heart disease. Patients with coronary artery disease, any cardiomyopathies including arrhythmogenic right ventricular cardiomyopathy/dysplasia (ARVC/D),¹³ Brugada syndrome,¹⁴ catecholaminergic polymorphic ventricular tachycardia,¹⁵ or long or short QT syndrome^{4,16} were excluded. The control group

consisted of 276 age- and gender-matched healthy subjects who were selected from among 7110 subjects who had routine health care examinations (12-leads ECG, blood test, chest X-ray film, and physical examinations) at our hospital health care centre between 2007 and 2009. The subjects with an abnormal 12-lead ECG (i.e. any arrhythmias, wide QRS complex, ST-segment elevation, T-wave inversion, QT interval abnormality, or Brugada-type ECG), blood test results, chest X-ray films, and physical examinations were excluded.

Definition of J-waves and analysis of the electrocardiogram parameters

The presence of J-waves during sinus rhythm (SR) was investigated in all the patients and control subjects. In the study patients, a 12-lead ECG was recorded after withdrawal of all antiarrhythmic drugs for at least five half-lives both 1–3 days before and 1–3 days after the RFCA. To blind the ECG interpreters to the patient grouping and patient information, all tracings were scanned and coded. Segments showing extra-systoles were not used. All scanned ECGs were analysed by two independent cardiologists in a random order and any controversial interpretations were re-discussed with a third observer. As previously described,^{1–8,17–19} the J-waves were defined as an

elevation of the J point noted as either a QRS slurring or notching of ≥ 0.1 mV in ≥ 2 contiguous leads in the inferior leads (II, III, aVF), or a lateral (I, aVL, V4–V6) distribution (Figures 1–3). Other ECG parameters, including the PR interval, QRS duration, and QT interval corrected for the heart rate (QTc) during stable SR at baseline were measured in lead V2. The QTc interval was calculated after a correction for the heart rate with Bazett's formula.

Clinically, documented ventricular arrhythmias recorded by Holter recordings or ECG monitoring in the idiopathic RVOT–VT/PVC patients were analysed in terms of the coupling interval of the VT/PVCs (ms), tachycardia CL (ms), and form of the ventricular arrhythmias. The form of the ventricular arrhythmias was divided into the following criteria: (i) PVCs were defined as isolated or two consecutive ectopic ventricular beats, (ii) non-sustained VT was defined as >3 consecutive beats and which terminated spontaneously within 30 s, (iii) sustained VT was defined as VT lasting ≥ 30 s, and (iv) VF was defined as a polymorphic ventricular tachyarrhythmia with haemodynamic decompensation requiring direct cardioversion for termination.

Comparison between idiopathic right ventricular outflow tract-ventricular tachycardia/pre-mature ventricular contractions patients with and without J-waves

Based on the presence or absence of J-waves during SR in the 12-lead ECG before the RFCA, the idiopathic RVOT–VT/PVC patients were divided into two groups: the J-RVOT–VT/PVC group and non-J-RVOT–VT/PVC group. The patients' clinical characteristics, ECG parameters during both SR and RVOT–VT/PVCs, data from electro-physiological study, outcome of the RFCA, J-waves' appearance after the RFCA, and the follow-up data were compared between the two groups.

Statistical analysis

Continuous variables were expressed as the mean \pm SD, and categorical variables were presented as the number and percent in each group. The prevalence of J-waves between the idiopathic RVOT–VT/PVC patients and control subjects was assessed by a conditional logistic regression analysis. A comparison of the continuous variables between the J-RVOT–VT/PVC group and non-J-RVOT–VT/PVC group was drawn by means of a Student's t-test. Categorical variables were compared using a χ^2 analysis with a Yates' correction if necessary. A *P* value <0.05 was considered significant (two-tailed).

Results

Prevalence of J-waves

Among the total of 138 RVOT–VT/PVC patients, six patients (four males) were excluded from the following analysis because of other coexisting ECG abnormalities [atrial fibrillation (1), second-degree atrio-ventricular block (1), sick sinus syndrome (1), and right bundle branch block (3)]. Another four patients (three males) demonstrated a J point elevation in the right pre-cordial leads (V1–3). Those four patients were also excluded from the following analysis in order to avoid any potential Brugada syndrome or ARVC/D.

J-waves were more common in the idiopathic RVOT–VT/PVC patients than among the matched control subjects [$n = 56$ (40) vs. $n = 46$ (16%), the odds ratio (OR) = 3.32, 95% confidence interval (CI) = 2.09–5.28, $P < 0.001$].

Comparison of the clinical, electrocardiographic, and electrophysiological characteristics between the J-right ventricular outflow tract-ventricular tachycardia/pre-mature ventricular contractions group and non-J-right ventricular outflow tract-ventricular tachycardia/pre-mature ventricular contractions group

Table 1 shows the comparison of the clinical parameters between the J-RVOT–VT/PVC group and non-J-RVOT–VT/PVC group. The patients in the two groups were of a similar age and gender. Prior episodes of syncope were more frequent in the J-RVOT–VT/PVC group than in the Non-J-RVOT–VT/PVC group (25 vs. 2% $P < 0.001$). The comparisons of the clinical ECG characteristics between the two groups are shown in Table 2. Isolated PVCs were a more common finding in the non-J-RVOT–VT/PVC group (23 vs. 47% $P < 0.01$). On the other hand, sustained VT was documented more frequently in the J-RVOT–VT/PVC group than in the non-J-RVOT–VT/PVC group (25 vs. 5% $P < 0.01$) (Figure 2). We could not document any VF in any of the patients. The coupling intervals of the initiating VT or PVCs did not differ between the two groups. However, the CL of the spontaneous VT was much shorter in the J-RVOT–VT/PVC group than in the non-J-RVOT–VT/PVC group (302 ± 57 vs. 351 ± 58 ms, $P < 0.001$) (Figure 3). The heart rate, PR interval, QRS duration, and QTc during SR did not differ statistically.

In all patients, no VF was induced by programmed electrical stimulation, and endocardial mapping represented no local abnormal electrograms, including fragmented or delayed potentials. Although four patients in the J-RVOT–VT/PVC group required rapid ventricular electrical stimulation to induce their clinical RVOT–VT/PVCs (Figure 2A), we could not demonstrate any electro-physiological evidence of a reentrant VT mechanism. No one in the non-J-RVOT–VT/PVC group needed any electrical ventricular stimulation to induce their clinical VT/PVCs during the electrophysiological study. No significant difference was observed regarding the success rate of the RFCA between the two groups (Table 2). After the RFCA, no J-waves were recorded in five patients in the J-RVOT–VT/PVC group. No one in the non-J-RVOT–VT/PVC group developed any J-waves after the RFCA.

The follow-up data were obtained in all patients in the J-RVOT–VT/PVC group and in 69 (95%) in the non-J-RVOT–VT/PVC group at our outpatient clinic. Three patients in the non-J-RVOT–VT/PVC group were referred to other institutions. No deaths were observed in any of the patients during the follow-up period (median of 12 months, interquartile range 4–25 months).

Discussion

To the best of our knowledge this is the first report showing the relationship between J-waves and idiopathic RVOT–VT/PVCs. The main findings in this study were as follows: (i) The prevalence of J-waves was 40% in the idiopathic RVOT–VT/PVC patients referred for RFCA in our institution, which was higher compared

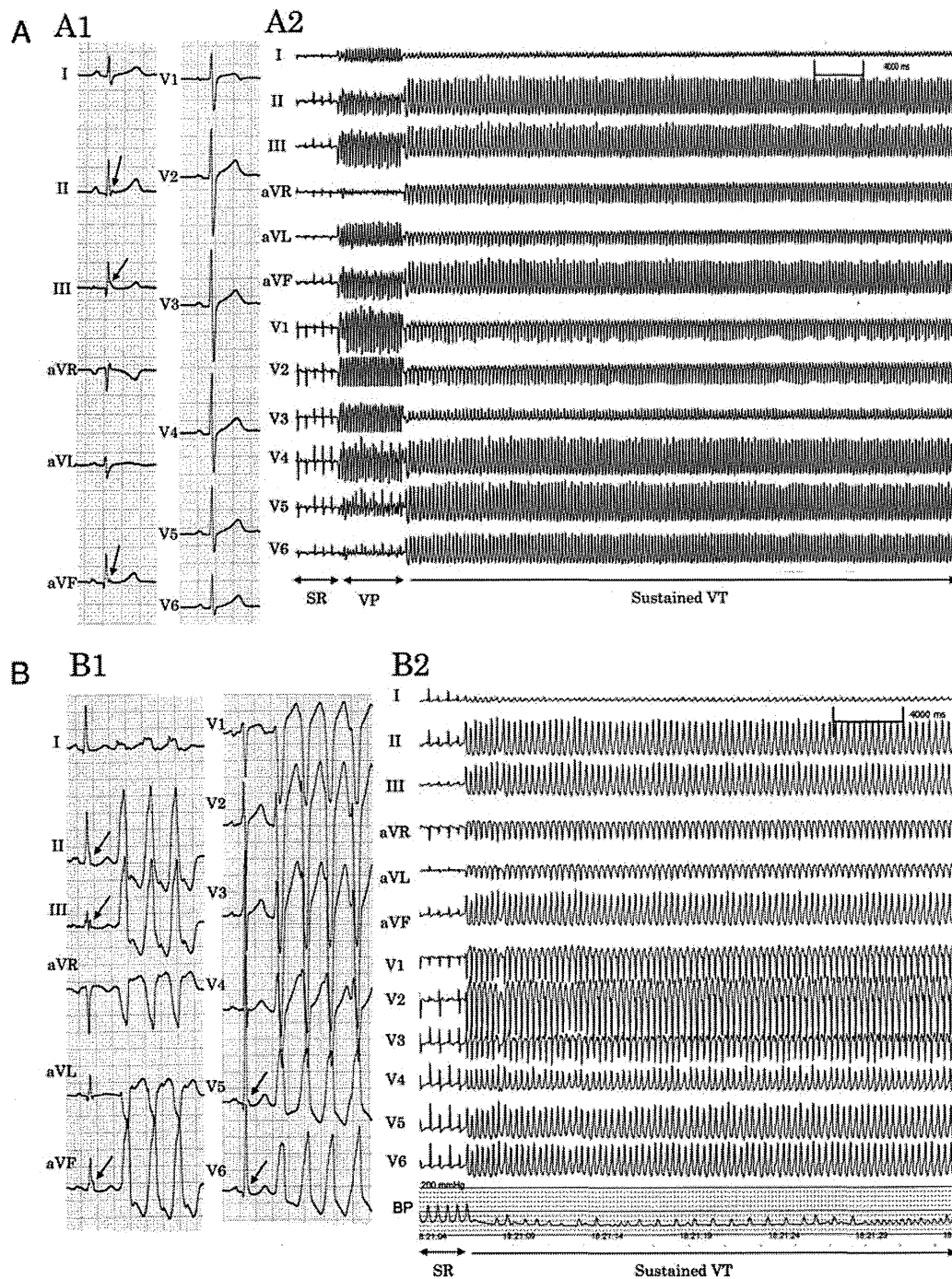


Figure 2 Two representative male patients with idiopathic right ventricular outflow tract-ventricular tachycardia associated with J-waves. (A) The 12-lead electrocardiograms in a 53-year-old male. (A1) The 12-lead electrocardiogram demonstrates the J-waves (QRS notching) in the inferior leads (arrow) during sinus rhythm. (A2) The 12-lead electrocardiogram during an electrophysiological study. The sustained ventricular tachycardia was induced by rapid ventricular pacing. (B) The 12-lead electrocardiograms in a 56-year-old male who suffered from repetitive syncopal episodes. (B1) The 12-lead electrocardiogram demonstrates the J-waves (QRS notching in the inferior leads and QRS slurring in V5–6: arrow), and non-sustained ventricular tachycardia with a left bundle branch block and inferior-axis deviation. (B2) The 12-lead electrocardiogram during an electrophysiological study. The sustained ventricular tachycardia appeared spontaneously with rapid lowering of the blood pressure. Radiofrequency catheter ablation of the ventricular tachycardia origin located in the right ventricular outflow tract completely eliminated the ventricular tachycardia in both patients.

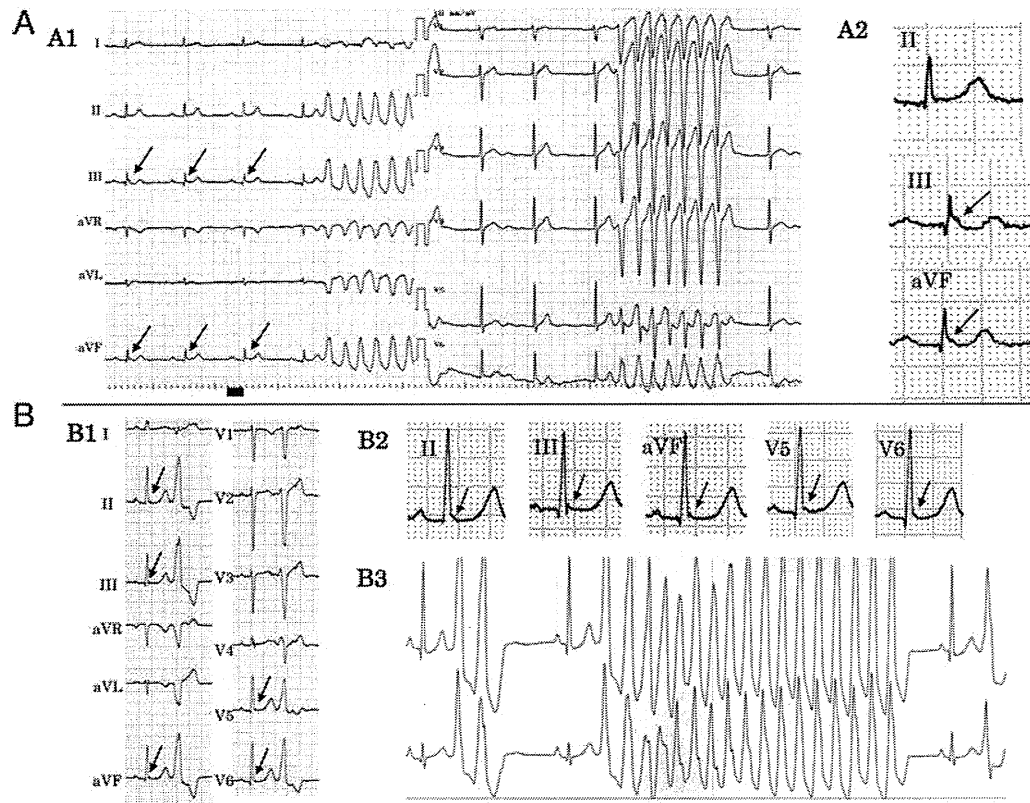


Figure 3 Two representative female patients in the J-right ventricular outflow tract-ventricular tachycardia/pre-mature ventricular contraction group. (A) A 42-year-old female. A1 and A2 show the baseline 12-lead electrocardiograms. The electrocardiogram demonstrates the J-waves (QRS notching) in the inferior leads (arrow) during sinus rhythm and rapid non-sustained ventricular tachycardia (cycle length=220 ms). (B) A 16-year-old female. B1 and B2 show the baseline electrocardiograms. The 12-lead electrocardiogram demonstrates the J-waves (QRS notching) in the inferior leads and in V5–6 (arrow) during sinus rhythm. (B3) The holter electrocardiogram in the same patient shows a very rapid non-sustained ventricular tachycardia (cycle length = 190 ms). Radiofrequency catheter ablation of the ventricular tachycardia origin in the right ventricular outflow tract completely eliminated the ventricular tachycardia in both patients.

Table 1 Comparison of the clinical characteristics between the J-right ventricular outflow tract-ventricular tachycardia/pre-mature ventricular contraction group and non-J-right ventricular outflow tract-ventricular tachycardia/pre-mature ventricular contraction group

Variables	J-RVOT-VT/ PVC group (n = 56)	Non-J-RVOT-VT/ PVC group (n = 72)	P value
Age (year)	44 ± 15	43 ± 15	0.32
Male gender	35% (n = 20)	25% (n = 18)	0.18
FH	5% (n = 3)	1% (n = 1)	0.44
Syncope	25% (n = 14)	2% (n = 2)	<0.001
Pre-syncope	14% (n = 8)	13% (n = 10)	0.84

FH, family history of sudden death.

with that in the healthy matched control subjects, (ii) idiopathic RVOT-VT/PVC patients associated with J-waves had a significantly higher incidence of sustained VT, shorter VT CL, and more episodes of syncope than did the idiopathic RVOT-VT/PVC patients without J-waves, and (iii) No patients demonstrated any VF or sudden death in the clinical course.

The presence of J-waves is a common ECG finding. It is present in 2–13% of the general population and usually is considered as a normal variant due to its benign long-term prognosis.^{1–4,8,17} However, recent clinical studies have reported an association between J-waves and idiopathic VF.^{1–3} Some studies have also suggested a high prevalence and arrhythmogenic significance of J-waves in various underlying arrhythmogenic situations (i.e. short QT syndrome,⁴ ARVD/C,⁵ chronic coronary artery disease,⁷ and Wolff–Parkinson–White syndrome¹⁸). On the other hand, idiopathic RVOT-VT/PVCs are the most common and usually are benign ventricular arrhythmias in patients without structural heart disease.^{9,10} It remains unknown as to whether or not the presence of J-waves affects the arrhythmogenicity of idiopathic RVOT-VT/

Table 2 Comparison of the clinical electrocardiogram characteristics and ablation outcome between the J-right ventricular outflow tract–ventricular tachycardia/pre-mature ventricular contraction group and non-J-right ventricular outflow tract–ventricular tachycardia/pre-mature ventricular contraction group

Variables	J-RVOT–VT/ PVC group (n = 56)	Non-J-RVOT– VT/PVC group (n = 72)	P value
Presenting arrhythmia			
PVCs	23% (n = 13)	47% (n = 34)	<0.01
Non-sustained VT	51% (n = 29)	47% (n = 34)	0.60
Sustained VT	25% (n = 14)	5% (n = 4)	<0.01
VF	0% (n = 0)	0% (n = 0)	
CL of VT/PVCs (ms)	444 ± 89	452 ± 85	0.61
CL of VT (ms)	302 ± 57 (n = 43)	351 ± 58 (n = 38)	<0.001
Parameters during sinus rhythm			
Heart rate (bpm)	65 ± 8	66 ± 12	0.31
QRS duration (ms)	54 ± 8	53 ± 9	0.62
PR interval (ms)	177 ± 20	177 ± 20	0.92
QTc (ms)	397 ± 23	399 ± 22	0.71
Successful RFCA	94% (n = 53)	90% (n = 65)	0.56

CL, coupling interval; CL, cycle length; PVCs, pre-mature ventricular contractions; QTc, QT interval corrected for heart rate with Bazett's formula; RFCA, radiofrequency catheter ablation; VF, ventricular fibrillation; VT, ventricular tachycardia.

PVCs. In the present study the prevalence of J-waves was surprisingly high (40%) in the idiopathic RVOT–VT/PVC patients referred for RFCA. We speculate that this high percentage of J-waves may represent an enhanced arrhythmogenicity in these patients. Patients with symptomatic and risky idiopathic RVOT–VT/PVCs are more likely to be referred for RFCA. Indeed, there was an intriguing correlation between the idiopathic RVOT–VT/PVC patients and J-waves with regard to sustained VT, short VT CL, and syncope.

On the other hand, we could not detect any documented VF in the present study cohort. This result is not surprising because idiopathic RVOT–VT/PVCs are usually benign.^{9,10} Our data suggest that the significance of J-waves in idiopathic RVOT–VT/PVC patients may be limited in terms of the overall prognosis and occurrence of VF. However, some recent reports have shown that idiopathic RVOT–VT/PVCs occasionally cause VF or sudden death ('malignant' idiopathic RVOT–VT/PVCs).^{20,21} The mechanism of the malignant form of idiopathic RVOT–VT/PVCs is unknown. Moreover, the electrophysiological mechanisms of the arrhythmogenesis related to J-waves have not been established. There is controversy over whether the pathogenesis of J-waves is related to an early ventricular repolarization abnormality or ventricular depolarization abnormality.³ In experimental studies, Antzelevitch and co-workers^{22–24} proposed that an epicardial–endocardial heterogeneity of the repolarization was responsible for J-waves observed in patients with idiopathic VF as well as

Brugada syndrome. Further, delayed after depolarizations (DADs) and triggered activity are believed to be the underlying mechanism of idiopathic RVOT–VT/PVCs.^{10,11} There have been no clinical studies explaining the direct link between the increased dispersion of ventricular repolarization and the DAD-induced triggered activity. However, Antzelevitch and co-workers^{25,26} demonstrated that DAD-induced triggered beats originated in the epicardium, leading to a reversal of the direction of the activation (from the epicardium to the endocardium instead the normal endocardial to epicardial activation), leads to a dramatic increase in the transmural dispersion of the repolarization. They speculated that DADs originating from the RVOT-epicardium not only initiate VT but also create the substrate for reentry by increasing the dispersion of the ventricular repolarization.^{25,26} Although previous studies reporting 'malignant' idiopathic RVOT–VT/PVCs did not mention about the presence of J-waves in their patient series, some clinical features are overlapping between the 'malignant' idiopathic RVOT–VT/PVCs reported previously²⁰ and the idiopathic RVOT–VT/PVCs associated with J-waves in the present study (i.e. shorter tachycardia CL and more episodes of syncope). We speculate that the presence of J-waves may reflect a potential propensity of ventricular proarrhythmias even in idiopathic RVOT–VT/PVCs patients. Although the proposed mechanism of sudden cardiac arrest associated with J-waves would suggest that these patients should present with VF, the exact mechanisms are yet to be elucidated. Some investigators have described an association between monomorphic VT and the presence of J-waves.^{6–8,12} Numerous reports have been published on patients with Brugada syndrome who have presented with monomorphic VT.^{27–29} The mechanisms and clinical implications of coexisting monomorphic VT and VF in Brugada syndrome also have not been clarified. Further clinical and experimental studies are needed to clarify the significance and risk of idiopathic VT/PVCs associated with underlying proarrhythmic situations such as J-waves in the inferior-lateral leads or Brugada pattern ECGs.

Study limitations

The present study had several limitations. First, this study was a single-centre, retrospective analysis. A further prospective evaluation is needed in a larger study population. Secondly, the present study cohort had a potential referral bias, because the patients with symptomatic and high-risk RVOT–VT/PVCs are more likely to be referred for RFCA, whereas asymptomatic patients are more likely to be treated conservatively. Therefore, we could not confirm the true prevalence of J-waves in the overall idiopathic RVOT–VT/PVC patients with this study design. Thirdly, all patients underwent a 12-lead ECG at least twice before and after the RFCA; however, the day-to-day variability in the ECG patterns should have been evaluated using more frequent ECG recordings. Fourthly, all patients and control subjects in the present study were Japanese. We could not analyse the relationship between the prevalence of J-waves and the genetic/ethnic differences. Very recently, an epidemiologic study in the Japanese population revealed that J-waves were common ECG findings, yielding a positive rate of 23.9% during the follow-up.¹⁹ It is possible that the high prevalence of J-waves in the present study reflected a genetic characteristic.

Conclusions

There was a high prevalence of J-waves in the idiopathic RVOT–VT/PVC patients referred for RFCA. Although patients with idiopathic RVOT arrhythmias associated with J-waves might have a more enhanced arrhythmogenicity than those without J-waves, the significance of those J-waves was limited in terms of the prognosis and VF. Further clinical and experimental studies are needed to clarify the clinical and electrophysiological relationship between the J-waves and idiopathic RVOT–VT/PVCs.

Conflict of interest: none declared.

References

- Haïssaguerre M, Derval N, Sacher F, Jesel L, Deisenhofer I, de Roy L et al. Sudden cardiac arrest associated with early repolarization. *N Engl J Med* 2008;**358**: 2016–23.
- Rosso R, Kogan E, Belhassen B, Rozovski U, Scheinman MM, Zeltser D et al. J-point elevation in survivors of primary ventricular fibrillation and matched control subjects: incidence and clinical significance. *J Am Coll Cardiol* 2008;**52**:1231–8.
- Abe A, Ikeda T, Tsukada T, Ishiguro H, Miwa Y, Miyakoshi M et al. Circadian variation of late potentials in idiopathic ventricular fibrillation associated with J waves: insights into alternative pathophysiology and risk stratification. *Heart Rhythm* 2010; **7**:675–82.
- Watanabe H, Makiyama T, Koyama T, Kannankeril PJ, Seto S, Okamura K et al. High prevalence of early repolarization in short QT syndrome. *Heart Rhythm* 2010;**7**:647–52.
- Peters S, Selbig D. Early repolarization phenomenon in arrhythmogenic right ventricular dysplasia-cardiomyopathy and sudden cardiac arrest due to ventricular fibrillation. *Europace* 2008;**10**:1447–9.
- Merchant FM, Noseworthy PA, Weiner RB, Singh SM, Ruskin JN, Reddy VY. Ability of terminal QRS notching to distinguish benign from malignant electrocardiographic forms of early repolarization. *Am J Cardiol* 2009;**104**:1402–6.
- Patel RB, Ng J, Reddy V, Chokshi M, Parikh K, Subacius H et al. Early repolarization associated with ventricular arrhythmias in patients with chronic coronary artery disease. *Circ Arrhythm Electrophysiol* 2010;**3**:489–95.
- Cappato R, Furlanello F, Giovinazzo V, Infusino T, Lupo P, Pittalis M et al. J wave, QRS slurring, and ST elevation in athletes with cardiac arrest in the absence of heart disease: marker of risk or innocent bystander? *Circ Arrhythm Electrophysiol* 2010;**3**:305–11.
- Zipes DP, Camm AJ, Borggrefe M, Buxton AE, Chaitman B, Fromer M et al. ACC/AHA/ESC 2006 guidelines for management of patients with ventricular arrhythmias and the prevention of sudden cardiac death: a report of the American College of Cardiology/American Heart Association Task Force and the European Society of Cardiology Committee for Practice Guidelines. *Europace* 2006;**8**: 746–837.
- Ghanbari H, Schmidt M, Machado C, Daccarett M. Catheter ablation of ventricular tachycardia in structurally normal hearts. *Expert Rev Cardiovasc Ther* 2010;**8**: 651–61.
- Yamashina Y, Yagi T, Namekawa A, Ishida A, Sato H, Nakagawa T et al. A case of sudden cardiac death during observation for idiopathic left bundle branch block and inferior axis deviation type premature ventricular contractions and J waves in inferior leads. *J Sendai City Hosp* 2010;**30**:71–4. (in Japanese).
- Ozeke O, Aras D, Celenk MK, Devenci B, Yildiz A, Topaloglu S et al. Exercise-induced ventricular tachycardia associated with J point ST-segment elevation in inferior leads in a patient without apparent heart disease: a variant form of Brugada syndrome? *J Electrocardiol* 2006;**39**:409–12.
- Cox MG, van der Smagt JJ, Noorman M. Arrhythmogenic right ventricular dysplasia/cardiomyopathy diagnostic task force criteria: impact of new task force criteria. *Circ Arrhythm Electrophysiol* 2010;**3**:126–33.
- Brugada P, Brugada J. Right bundle branch block, persistent ST segment elevation and sudden cardiac death: a distinct clinical and electrocardiographic syndrome. A multicenter report. *J Am Coll Cardiol* 1992;**20**:1391–6.
- Leenhardt A, Lucet V, Denjoy I, Grau F, Ngoc DD, Coumel P. Catecholaminergic polymorphic ventricular tachycardia in children. A 7-year follow-up of 21 patients. *Circulation* 1995;**91**:1512–9.
- Moss AJ, Schwartz PJ, Crampton RS, Locati E, Carleen E. The long QT syndrome: a prospective international study. *Circulation* 1985;**71**:17–21.
- Sinner MF, Reinhard W, Müller M, Beckmann BM, Martens E, Perz S et al. Association of early repolarization pattern on ECG with risk of cardiac and all-cause mortality: a population-based prospective cohort study (MONICA/KORA). *PLoS Med* 2010;**7**:e1000314.
- Mizumaki K, Nishida K, Iwamoto J, Nakatani Y, Yamaguchi Y, Sakamoto T et al. Early repolarization in Wolff–Parkinson–White syndrome: prevalence and clinical significance. *Europace* 2011;**13**:1195–1200.
- Daisuke Haruta, Kiyotaka Matsuo, Akira Tsuneto, Shinichiro Ichimaru, Ayumi Hida, Nobuko Sera et al. Incidence and prognostic value of early repolarization pattern in the 12-lead electrocardiogram. *Circulation* 2011;**123**:2931–7.
- Noda T, Shimizu W, Taguchi A, Aiba T, Satomi K, Suyama K et al. Malignant entity of idiopathic ventricular fibrillation and polymorphic ventricular tachycardia initiated by premature extrasystoles originating from the right ventricular outflow tract. *J Am Coll Cardiol* 2005;**46**:1288–94.
- Viskin S, Rosso R, Rogowski O, Belhassen B. The 'short-coupled' variant of right ventricular outflow ventricular tachycardia: a not-so-benign form of benign ventricular tachycardia? *J Cardiovasc Electrophysiol* 2005;**16**:912–6.
- Gussak I, Antzelevitch C. Early repolarization syndrome: clinical characteristics and possible cellular and ionic mechanisms. *J Electrocardiol* 2000;**33**:299–309.
- Yan GX, Antzelevitch C. Cellular basis for the Brugada syndrome and other mechanisms of arrhythmogenesis associated with ST-segment elevation. *Circulation* 1999;**100**:1660–6.
- Yan GX, Antzelevitch C. Cellular basis for the electrocardiographic J wave. *Circulation* 1996;**93**:372–9.
- Fish JM, Di Diego JM, Nesterenko V, Antzelevitch C. Epicardial activation of left ventricular wall prolongs QT interval and transmural dispersion of repolarization: implications for biventricular pacing. *Circulation* 2004;**109**:2136–42.
- Viskin S, Antzelevitch C. The cardiologists' worst nightmare sudden death from 'benign' ventricular arrhythmias. *J Am Coll Cardiol* 2005;**46**:1295–7.
- Shimada M, Miyazaki T, Miyoshi S, Soejima K, Hori S, Mitamura H et al. Sustained monomorphic ventricular tachycardia in a patient with Brugada syndrome. *Jpn Circ J* 1996;**60**:364–70.
- Dinckal MH, Davutoglu V, Akdemir I, Soyuncu S, Kirilmaz A, Aksoy M. Incessant monomorphic ventricular tachycardia during febrile illness in a patient with Brugada syndrome: fatal electrical storm. *Europace* 2003;**5**: 257–61.
- Chinushi M, Furushima H, Hosaka Y, Izumi D, Aizawa Y. Ventricular fibrillation and ventricular tachycardia triggered by late-coupled ventricular extrasystoles in a Brugada syndrome patient. *Pacing Clin Electrophysiol* 2011; **34**:e1–5.

Research Article

Short-Term Effects of Acupuncture on Open-Angle Glaucoma in Retrobulbar Circulation: Additional Therapy to Standard Medication

**Shin Takayama,¹ Takashi Seki,¹ Toru Nakazawa,² Naoko Aizawa,²
Seri Takahashi,² Masashi Watanabe,¹ Masayuki Izumi,¹ Soichiro Kaneko,¹
Tetsuharu Kamiya,¹ Ayane Matsuda,¹ Akiko Kikuchi,¹ Tomoyuki Yambe,³
Makoto Yoshizawa,⁴ Shin-ichi Nitta,³ and Nobuo Yaegashi¹**

¹Department of Traditional Asian Medicine, Graduate School of Medicine, Tohoku University,
1-1 Seiryō-machi, Aoba-ku, Sendai, Miyagi 980-8574, Japan

²Department of Ophthalmology and Visual Science, Graduate School of Medicine, Tohoku University, Sendai 980-8574, Japan

³Institute of Development, Aging and Cancer, Tohoku University, Sendai 980-8575, Japan

⁴Research Division on Advanced Information Technology, Cyberscience Center, Tohoku University, Japan

Correspondence should be addressed to Takashi Seki, t-seki@m.tohoku.ac.jp

Received 29 October 2010; Revised 7 December 2010; Accepted 11 January 2011

Copyright © 2011 Shin Takayama et al. This is an open access article distributed under the Creative Commons Attribution License, which permits unrestricted use, distribution, and reproduction in any medium, provided the original work is properly cited.

Background. The relation between glaucoma and retrobulbar circulation in the prognosis has been indicated. **Purpose.** To investigate the effects of acupuncture on retrobulbar circulation in open-angle glaucoma (OAG) patients. **Methods.** Eleven OAG patients (20 eyes with OAG) who were treated by topical antiglaucoma medications for at least 3 months were enrolled. Acupuncture was performed once at acupoints BL2, M-HN9, ST2, ST36, SP6, KI3, LR3, GB20, BL18, and BL23 bilaterally. Retrobulbar circulation was measured with color Doppler imaging, and intraocular pressure (IOP) was also measured at rest and one hour after rest or before and after acupuncture. **Results.** The Δ value of the resistive index in the short posterior ciliary artery ($P < .01$) and the Δ value of IOP ($P < .01$) were decreased significantly by acupuncture compared with no acupuncture treatment. **Conclusions.** Acupuncture can improve the retrobulbar circulation and IOP, which may indicate the efficacy of acupuncture for OAG.

1. Introduction

Glaucoma is one of the causes of blindness [1] and the Tajimi Study showed that the prevalence of primary open-angle glaucoma (OAG) was 3.9% in Japan [2]. The main treatment strategy of glaucoma is to control the intraocular pressure (IOP) [3]. Although IOP reduction is currently the main target for the treatment of glaucoma, treatment modalities that enhance retrobulbar hemodynamics in addition to reducing IOP may have a beneficial effect on the glaucoma therapy. It has been reported that glaucoma is associated with reduction in the blood flow velocity and elevation of the resistive index (RI) in the retrobulbar vessels [4–7]. It has also been reported that patients with OAG have impaired hemodynamics in ophthalmic circulation [8–10].

The impaired ocular circulation contributes to the progression of glaucomatous damage [11–13]. Therefore, new drugs or interventions that improve ocular hemodynamics may be preferable.

Recently, acupuncture has been widely applied to treat several conditions such as neck pain, shoulder pain, lumbar pain, headache, and hypertension in Asian and Western countries, and it has also been found to be effective for many conditions in several randomized trials [14–20]. Acupuncture has also been used for the treatment of ocular diseases, including glaucoma, in traditional Chinese medicine [21]. We have shown that acupuncture therapy added to the standard medication could affect the IOP level in eyes with normal-tension glaucoma [22], and several other studies have demonstrated that

acupuncture improves choroidal blood flow in the eye [23–25].

We have already reported that color Doppler imaging (CDI) by ultrasound is suitable for measuring the blood flow change in several organs during traditional Chinese medicine therapy [26–30]. The real-time and noninvasive hemodynamic measurement with CDI has been applied for measuring the retrobulbar vessel hemodynamics, and the reproducibility has already been shown [31]. In this study, we evaluate the hemodynamic changes in retrobulbar vessels by CDI to investigate the effect of acupuncture on OAG eyes.

2. Subjects

After the ethics committee approved the study, 11 patients diagnosed with OAG (20 eyes with OAG) were enrolled in this study. The patients received standard medical treatment for at least 3 months. The patients who had an experience of laser trabeculoplasty, any ocular surgery, or inflammation within the past year were excluded in the present study.

3. Methods

3.1. Acupuncture. On the trial days, the patients arrived under regular medications. They received acupuncture therapy as follows in the morning. The acupoints were selected on the basis of the principles of traditional Chinese medicine. Acupuncture was performed for 15 min using disposable stainless steel needles (0.16 mm or 0.20 mm × 40 mm; Seirin Co. Ltd., Shizuoka, Japan) at acupoints Cuanzhu (BL2), Taiyang (M-HN9), Sibai (ST2), Zusanli (ST36), Sanyinjiao (SP6), Taixi (KI3), and Taichong (LR3) bilaterally while the patient was in the supine position and at acupoints Fengchi (GB20), Ganshu (BL18), and Shenshu (BL23) bilaterally while the patient was in the prone position for 15 min. Each needle was simply inserted without any intention of eliciting specific responses (e.g., de-qi feelings) to a depth of approximately 20 mm at acupoints ST36, SP6, KI3, GB20, BL18, and BL23. For acupoints BL2, M-HN9, ST2, and LR3, the needles were inserted to a depth of approximately 3–10 mm. Neither needle manipulation techniques nor other auxiliary interventions were used. Five licensed acupuncturists and one physician-acupuncturist with over 5 years of acupuncture experience administered the acupuncture treatment.

3.2. Measurements. To minimize the effects of diurnal variation, all measurements were recorded at the same time of the day (between 10 AM and 11 AM) for each patient by the same examiner. As a control, the subjects received the measurements of the systemic hemodynamics, retrobulbar vessel hemodynamics, and IOP that were performed at rest and one hour after rest. One month later, they received the same measurements before and after acupuncture treatment. The systemic hemodynamics was measured by an oscillometer and the hemodynamics in retrobulbar vessels was measured by ultrasound (LOGIQ e, GE Healthcare, Tokyo, Japan). The ultrasound measurements were performed after 10-minute

TABLE 1: Characteristic data of the patients with open-angle glaucoma.

Variable	Value
Number of patients	11
Age (years)	63 ± 11
Sexuality (male, female)	(1, 10)
Number of eyes with glaucoma	20
Best corrected visual acuity	1.1 ± 0.3
Spherical equivalent (D)	−1.6 ± 3.2
Humphrey automated perimeter	
Mean deviation (dB)	−11.5 ± 7.8
Pattern standard deviation (dB)	10.2 ± 4.5
OCT RNFL thickness (μm)	70.5 ± 21.8
The number of topical medications	
None	1
One kind	4
Two kinds	1
More than three kinds	5

rest in an air-conditioned room, avoiding any pressure on the eye, with the patients in the supine position. CDI was performed with a 13 MHz linear transducer for retrobulbar vessels such as the ophthalmic artery (OA), central retinal artery (CRA), and short posterior ciliary artery (SPCA). The OA was examined approximately 20 mm behind the globe (Figure 1(a)), the CRA was examined within 5 mm of the retrolaminar portion of the optic nerve (Figure 1(b)), and the temporal SPCA was examined approximately 5–10 mm behind the globe (Figure 1(c)). All blood flow velocity waveforms were measured at the corrected Doppler angle. Resistive index (RI: (peak systolic velocity – end-diastolic velocity)/peak systolic velocity) was also measured in each retrobulbar vessel.

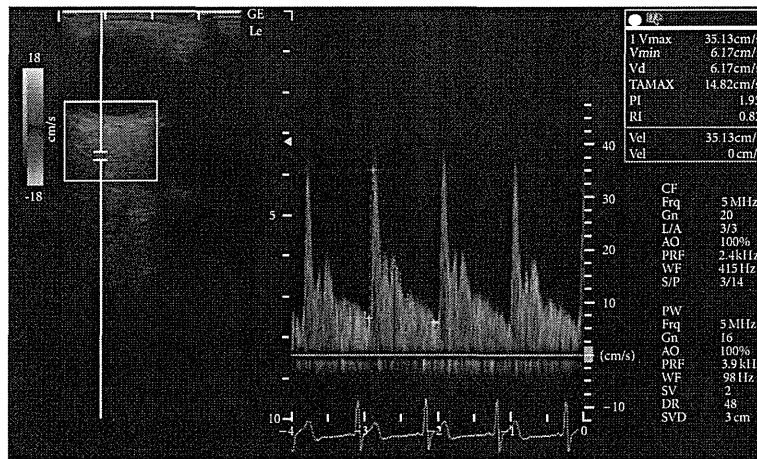
3.3. Statistical Analysis. Statistical analysis was performed with the SPSS software (version 16.0, SPSS Japan Inc., Tokyo, Japan). The parameters between before and after acupuncture or between control and acupuncture were compared by paired *t*-test.

4. Results

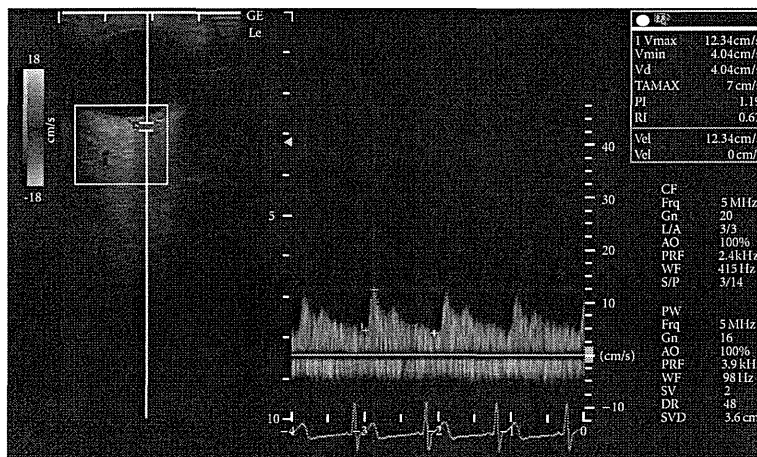
Table 1 shows the characteristics of the subjects. One male and ten female glaucoma patients with a mean age of 63 ± 11 years were observed. The systemic hemodynamic parameters including heart rate, blood pressure, and IOP are shown in Table 2. The blood pressure and heart rate did not change significantly by acupuncture.

The IOP level significantly decreased by acupuncture compared with before acupuncture ($P < .05$). The Δ value of IOP also significantly decreased by acupuncture compared with control ($P < .01$) (Table 2).

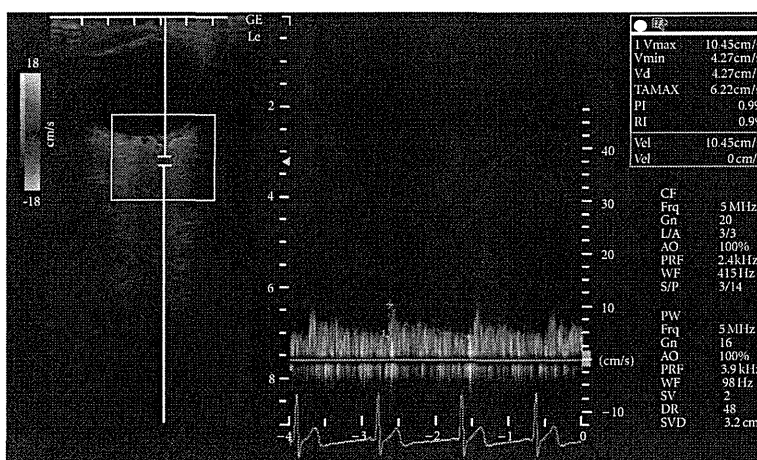
Retrobulbar vessel RI in the OA, CRA, and SPCA is shown in Table 3. The RI in the CRA and SPCA decreased



(a)



(b)



(c)

FIGURE 1: Horizontal scans by color Doppler imaging through the globe showing the (a) ophthalmic artery, (b) central retinal artery, and (c) short posterior ciliary artery.

TABLE 2: Blood pressure, heart rate, and intraocular pressure in control and acupuncture therapy. The values represent the mean and SD. * $P < .05$, ** $P < .01$ versus rest or before acupuncture. † $P < .05$, †† $P < .01$ versus control.

Parameter	Control			Acupuncture		
	Rest	After 1 hour	Δ value	Before	After	Δ value
Systole blood pressure (mm Hg)	116.4 \pm 10.0	119.8 \pm 7.6	3.4 \pm 7.4	124.5 \pm 12.9	122.6 \pm 9.7	-1.1 \pm 7.9
Diastolic blood pressure (mm Hg)	69.8 \pm 6.5	68.6 \pm 3.9	-1.0 \pm 9.4	74.5 \pm 5.4	72.0 \pm 2.9	-3.0 \pm 5.5
Heart rate (beats/min)	61.5 \pm 7.3	60.1 \pm 8.1	-2.5 \pm 3.8	61.7 \pm 8.5	60.3 \pm 10.4	-2.4 \pm 5.5
Intraocular pressure (mm Hg)	16.0 \pm 4.1	17.1 \pm 4.2**	1 \pm 0.9	17.0 \pm 5.0	16.0 \pm 4.3*	-1 \pm 1.9††

TABLE 3: Resistive index (RI) in the ophthalmic artery, central retinal artery, and short posterior ciliary artery. The values represent the mean and SD. * $P < .05$, ** $P < .01$ versus before acupuncture. † $P < .05$, †† $P < .01$ versus control.

Resistive index	Control			Acupuncture		
	Rest	After 1 hour	Δ value	Before	After	Δ value
Ophthalmic artery	0.74 \pm 0.04	0.75 \pm 0.05	0.006 \pm 0.037	0.74 \pm 0.04	0.74 \pm 0.04	-0.006 \pm 0.036
Central retinal artery	0.75 \pm 0.09	0.72 \pm 0.03	-0.027 \pm 0.085	0.72 \pm 0.05	0.68 \pm 0.04*	-0.036 \pm 0.059
Short posterior ciliary artery	0.68 \pm 0.05	0.68 \pm 0.04	0.004 \pm 0.038	0.67 \pm 0.04	0.64 \pm 0.06*	-0.032 \pm 0.054††

significantly by acupuncture compared with before acupuncture ($P < .05$). The Δ value of RI in the SPCA also significantly decreased by acupuncture compared with control ($P < .01$) (Table 3).

5. Discussion

To our best knowledge, this is the first report on hemodynamic change in retrobulbar vessels related to acupuncture in OAG eyes. The present findings suggest that acupuncture can alter vessel resistance in the SPCA, even though the eyes are treated with standard medications.

The OA originates from the internal carotid artery. The CRA and SPCA are the ocular branches of the OA [32]. The CRA supplies blood to the retina and SPCA, to the choroid. CDI by ultrasound is useful for the measurement of the blood flow in various vessels in real time. Since it is impossible to determine the diameter of very small retrobulbar vessels, CDI cannot directly measure blood flow volume. However, the decrease of the distal vascular resistance in the SPCA indicates an increase of the blood flow in the choroid. We have already reported that acupuncture could increase the blood flow volume in the upper limb without an increase in the cardiac output, and the increased reaction in the blood flow was mediated by the decrease in the vascular resistance on the basis of the decreased vascular tone [30]. The mechanisms by which acupuncture can alter retrobulbar vessel circulation are still unclear. However, it has been reported that the blood flow in the eye is controlled by sympathetic and parasympathetic nerves, and it is related with the release of nitric oxide or calcitonin gene-related peptide [33, 34]; it has also been reported that the regulation of regional blood flow by somatic afferent stimulation is based on somatoautonomic reflex mechanisms in the choroidal blood flow of the eyeball [34]. The hemodynamic changes in the SPCA by acupuncture may be related with these mechanisms. Reduced blood flow velocities and increased vascular resistance in the retrobulbar

arteries appear to be a risk factor for glaucoma progression [35–38]. Thus, acupuncture may be applied for additional therapy to treat OAG.

We should view these results cautiously because the present study was a case series study and intervention was provided only once. Longer observation of acupuncture therapy is needed to investigate the progression of glaucomatous damage associated with impaired ocular circulation.

6. Conclusions

The vessel resistance in the SPCA and the IOP level were decreased by acupuncture in OAG eyes. Acupuncture can affect the retrobulbar circulation and IOP despite the administration of standard medication. The present study implies the possibility that acupuncture is effective for OAG with standard medication.

Acknowledgment

This work was supported by Health and Labour Sciences Research Grants for Clinical Research from the Japanese Ministry of Health, Labour and Welfare.

References

- [1] K. Nakae, K. Masuda, T. Aneo et al., "Wagakuni ni okeru shiryokushougai no genjou," *Research Committee on Chorioretinal Degenerations and Optic Atrophy, the Ministry of Health, Labour and Welfare of Japan*, vol. 17, pp. 263–276, 2005.
- [2] A. Iwase, Y. Suzuki, M. Araie et al., "The prevalence of primary open-angle glaucoma in Japanese: the Tajimi study," *Ophthalmology*, vol. 111, no. 9, pp. 1641–1648, 2004.
- [3] R. N. Weinreb and P. Tee Khaw, "Primary open-angle glaucoma," *The Lancet*, vol. 363, no. 9422, pp. 1711–1720, 2004.
- [4] C. Akarsu and M. Y. K. Bilgili, "Color Doppler imaging in ocular hypertension and open-angle glaucoma," *Graefes*

- Archive for Clinical and Experimental Ophthalmology*, vol. 242, no. 2, pp. 125–129, 2004.
- [5] V. P. Costa, A. Harris, E. Stefánsson et al., “The effects of antiglaucoma and systemic medications on ocular blood flow,” *Progress in Retinal and Eye Research*, vol. 22, no. 6, pp. 769–805, 2003.
 - [6] H. J. Kaiser, A. Schoetzau, D. Stumpfig, and J. Flammer, “Blood-flow velocities of the extraocular vessels in patients with high-tension and normal-tension primary open-angle glaucoma,” *American Journal of Ophthalmology*, vol. 123, no. 3, pp. 320–327, 1997.
 - [7] S. J. A. Rankin, “Color Doppler imaging of the retrobulbar circulation in glaucoma,” *Survey of Ophthalmology*, vol. 43, no. 1, pp. S176–S182, 1999.
 - [8] I. Stalmans, A. Harris, S. Fieuws et al., “Color Doppler imaging and ocular pulse amplitude in glaucomatous and healthy eyes,” *European Journal of Ophthalmology*, vol. 19, no. 4, pp. 580–587, 2009.
 - [9] I. Janulevičienė, I. Sliesoraitytė, B. Siesky, and A. Harris, “Diagnostic compatibility of structural and haemodynamic parameters in open-angle glaucoma patients,” *Acta Ophthalmologica*, vol. 86, no. 5, pp. 552–557, 2008.
 - [10] N. Plange, M. Kaup, O. Arend, and A. Remky, “Asymmetric visual field loss and retrobulbar haemodynamics in primary open-angle glaucoma,” *Graefe’s Archive for Clinical and Experimental Ophthalmology*, vol. 244, no. 8, pp. 978–983, 2006.
 - [11] M. Satilmis, S. Orgül, B. Doubler, and J. Flammer, “Rate of progression of glaucoma correlates with retrobulbar circulation and intraocular pressure,” *American Journal of Ophthalmology*, vol. 135, no. 5, pp. 664–669, 2003.
 - [12] J. Schumann, S. Orgül, K. Gugleta, B. Dubler, and J. Flammer, “Interocular difference in progression of glaucoma correlates with interocular differences in retrobulbar circulation,” *American Journal of Ophthalmology*, vol. 129, no. 6, pp. 728–733, 2000.
 - [13] Y. Yamazaki and S. M. Drance, “The relationship between progression of visual field defects and retrobulbar circulation in patients with glaucoma,” *American Journal of Ophthalmology*, vol. 124, no. 3, pp. 287–295, 1997.
 - [14] X. Xu, “Acupuncture in an outpatient clinic in China: a comparison with the use of acupuncture in North America,” *Southern Medical Journal*, vol. 94, no. 1–10, pp. 813–816, 2001.
 - [15] V. Napadow and T. J. Kaptchuk, “Patient characteristics for outpatient acupuncture in Beijing, China,” *Journal of Alternative and Complementary Medicine*, vol. 10, no. 3, pp. 565–572, 2004.
 - [16] C. M. Witt, S. Jena, B. Brinkhaus, B. Liecker, K. Wegscheider, and S. N. Willich, “Acupuncture for patients with chronic neck pain,” *Pain*, vol. 125, no. 1–2, pp. 98–106, 2006.
 - [17] B. Brinkhaus, C. M. Witt, S. Jena et al., “Acupuncture in patients with chronic low back pain: a randomized controlled trial,” *Archives of Internal Medicine*, vol. 166, no. 4, pp. 450–457, 2006.
 - [18] D. Melchart, A. Streng, A. Hoppe et al., “Acupuncture in patients with tension-type headache: randomised controlled trial,” *British Medical Journal*, vol. 331, no. 7513, pp. 376–379, 2005.
 - [19] C. Witt, B. Brinkhaus, S. Jena et al., “Acupuncture in patients with osteoarthritis of the knee: a randomised trial,” *The Lancet*, vol. 366, no. 9480, pp. 136–143, 2005.
 - [20] K. Linde, A. Streng, S. Jürgens et al., “Acupuncture for patients with migraine: a randomized controlled trial,” *Journal of the American Medical Association*, vol. 293, no. 17, pp. 2118–2125, 2005.
 - [21] *Diseases of Eyes, Ears, Nose and Throat*, vol. 681, Eastland Press, Seattle, Wash, USA, 1981.
 - [22] M. Kurusu, K. Watanabe, T. Nakazawa et al., “Acupuncture For Patients With Glaucoma,” *Explore*, vol. 1, no. 5, pp. 372–376, 2005.
 - [23] S. Naruse, K. Mori, M. Kurihara et al., “Chorioretinal blood flow changes following acupuncture between thumb and forefinger,” *Journal of Japanese Ophthalmological Society*, vol. 104, no. 10, pp. 717–723, 2000.
 - [24] M. Shimura, S. Uchida, A. Suzuki, K. Nakajima, and Y. Aikawa, “Reflex choroidal blood flow responses of the eyeball following somatic sensory stimulation in rats,” *Autonomic Neuroscience*, vol. 97, no. 1, pp. 35–41, 2002.
 - [25] J. J. Steinle, D. Krizsan-Agbas, and P. G. Smith, “Regional regulation of choroidal blood flow by autonomic innervation in the rat,” *American Journal of Physiology*, vol. 279, no. 1, pp. R202–R209, 2000.
 - [26] S. Takayama, T. Seki, N. Sugita et al., “Radial artery hemodynamic changes related to acupuncture,” *Explore*, vol. 6, no. 2, pp. 100–105, 2010.
 - [27] S. Takayama, T. Seki, M. Watanabe et al., “Changes of blood flow volume in the superior mesenteric artery and brachial artery with abdominal thermal stimulation,” *Evidence-Based Complementary and Alternative Medicine*, vol. 17, pp. 1–9, 2009.
 - [28] S. Takayama, T. Seki, M. Watanabe et al., “The herbal medicine Daikenchuto increases blood flow in the superior mesenteric artery,” *Tohoku Journal of Experimental Medicine*, vol. 219, no. 4, pp. 319–330, 2009.
 - [29] S. Takayama, T. Seki, M. Watanabe et al., “The effect of warming of the abdomen and of herbal medicine on superior mesenteric artery blood flow—a pilot study,” *Forschende Komplementarmedizin*, vol. 17, no. 4, pp. 195–201, 2010.
 - [30] S. Takayama, T. Seki, M. Watanabe et al., “Brief effect of acupuncture on the peripheral arterial system of the upper limb and systemic hemodynamics in humans,” *Journal of Alternative and Complementary Medicine*, vol. 16, no. 7, pp. 707–713, 2010.
 - [31] E. T. Matthiessen, O. Zeitz, G. Richard, and M. Klemm, “Reproducibility of blood flow velocity measurements using colour decoded Doppler imaging,” *Eye*, vol. 18, no. 4, pp. 400–405, 2004.
 - [32] S. S. Hayreh and R. Dass, “The ophthalmic artery II: intra orbital course,” *The British Journal of Ophthalmology*, vol. 46, no. 3, pp. 165–185, 1962.
 - [33] A. K. Wiencke, H. Nilsson, P. J. Nielsen, and N. C. B. Nyborg, “Nonadrenergic noncholinergic vasodilation in bovine ciliary artery involves CGRP and neurogenic nitric oxide,” *Investigative Ophthalmology and Visual Science*, vol. 35, no. 8, pp. 3268–3277, 1994.
 - [34] M. Shimura, S. Uchida, A. Suzuki, K. Nakajima, and Y. Aikawa, “Reflex choroidal blood flow responses of the eyeball following somatic sensory stimulation in rats,” *Autonomic Neuroscience*, vol. 97, no. 1, pp. 35–41, 2002.
 - [35] D. Gherghel, S. Orgül, K. Gugleta, M. Gekkieva, and J. Flammer, “Relationship between ocular perfusion pressure and retrobulbar blood flow in patients with glaucoma with progressive damage,” *American Journal of Ophthalmology*, vol. 130, no. 5, pp. 597–605, 2000.
 - [36] O. Zeitz, P. Galambos, L. Wagenfeld et al., “Glaucoma progression is associated with decreased blood flow velocities in the short posterior ciliary artery,” *British Journal of Ophthalmology*, vol. 90, no. 10, pp. 1245–1248, 2006.

- [37] F. Galassi, A. Sodi, F. Ucci, G. Renieri, B. Pieri, and M. Baccini, "Ocular hemodynamics and glaucoma prognosis: a color Doppler imaging study," *Archives of Ophthalmology*, vol. 121, no. 12, pp. 1711–1715, 2003.
- [38] A. Martínez and M. Sánchez, "Predictive value of colour Doppler imaging in a prospective study of visual field progression in primary open-angle glaucoma," *Acta Ophthalmologica Scandinavica*, vol. 83, no. 6, pp. 716–722, 2005.

Comparison between Ultrasonic-Measurement-Integrated Simulation and Ordinary Simulation with Measured Upstream Velocity Condition

Shusaku SONE¹, Takaumi KATO¹, Kenichi FUNAMOTO², Toshiyuki HAYASE², Masafumi OGASAWARA³,
Takao JIBIKI³, Hiroshi HASHIMOTO³, Kouji MIYAMA³

1 Graduate School of Biomedical Engineering, Tohoku University, 6-6-4 Aramaki Aza Aoba, Aoba-ku, Sendai 980-8579, JAPAN

2 Institute of Fluid Science, Tohoku University, 2-1-1 Katahira, Aoba-ku, Sendai 980-8577, JAPAN

3 GE Healthcare Japan, 4-7-127 Asahigaoka, Hino 191-8503, JAPAN

sone@reynolds.ifs.tohoku.ac.jp

ABSTRACT

In this study, UMI simulation and ordinary simulation with several upstream velocity boundary conditions were performed for blood flow in a carotid artery. The error of the UMI simulation was found to be almost half that of the ordinary simulation with measured upstream velocity condition, showing better accuracy in reproducing the blood flow.

1. Introduction

Development and progression of cardiovascular diseases is closely related to hemodynamics. As a novel technique to reproduce a blood flow field for advanced diagnosis, the authors have proposed and developed ultrasonic-measurement-integrated (UMI) simulation [1]. This method employs unsteady computation with feedback of errors in Doppler velocities, which are velocity components in the ultrasound beam direction of the blood flow, between ultrasonic measurement and computation to make the numerical result converge to the actual blood flow field, even if the accurate velocity profile at the upstream boundary is unknown. To date, we have constructed a two-dimensional UMI simulation system (Fig. 1) and shown the relationships between hemodynamic parameters based on the wall shear stress and pathology by investigating a number of clinical data of the carotid artery [2].

However, in the previous study, the accuracy between the UMI simulation and the ordinary simulation with a measured upstream velocity boundary condition was not compared. Thus, in the present study, we performed UMI simulation and ordinary simulation with several upstream velocity boundary conditions for a blood flow in a carotid artery to compare the accuracy of the results.

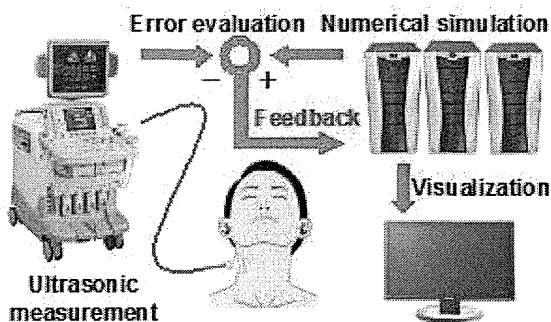


Fig. 1 Ultrasonic-Measurement-Integrated Simulation System

2. Method

The governing equations of UMI simulation are the Navier-Stokes equation (Eq. (1)) and the pressure equation (Eq. (2)) for incompressible and viscous fluid flow,

$$\rho \left(\frac{\partial \mathbf{u}}{\partial t} + (\mathbf{u} \cdot \nabla) \mathbf{u} \right) = \mu \Delta \mathbf{u} - \nabla p + \mathbf{f} \quad (1)$$

$$\Delta p = -\rho \nabla \cdot (\mathbf{u} \cdot \nabla) \mathbf{u} + \nabla \cdot \mathbf{f}, \quad (2)$$

where \mathbf{u} is the velocity vector, p is the pressure, t is time, ρ is the density, μ is the dynamic viscosity, and \mathbf{f} is the feedback signal. It is defined as an artificial body force proportional to the difference of Doppler velocities, V , between ultrasonic measurement and numerical simulation as follows:

$$\mathbf{f} = -K_v^* \frac{V_c - V_m}{U} \left(\frac{\rho U^2}{L} \right), \quad (3)$$

where K_v^* is the feedback gain (non-dimensional), U is the characteristic velocity, L is the characteristic length, and subscripts m and c represent the ultrasonic measurement and UMI simulation, respectively. The special case with $K_v^* = 0$ is the ordinary numerical simulation without feedback. The above governing equations were discretized by means of the finite volume method and were solved with the algorithm similar to the SIMPLER method.

The shape of the carotid artery was extracted by binarizing both time averaged color Doppler images and time averaged B mode images. The shape was then rotated so that the main direction of the blood flow would agree with the x -directional axis, and the computational grid was generated. The size of the computational grid is the same as the resolution of ultrasonic measurement, as $\Delta x = 280 [\mu\text{m}]$ and $\Delta y = 170 [\mu\text{m}]$, respectively. The objective was a blood flow in a carotid artery of an informed 76-years-old female patient. Ultrasound color Doppler images of 5 heart beats acquired with ultrasound diagnostic imaging equipment (LOGIQ7, GE Healthcare, JAPAN) with an

ultrasonic linear probe was used for analysis. The main frequency and repeated frequency were 5 MHz and 4.4 kHz, respectively. Feedback domain was set from 1/8 to 7/8 of the computational domain from the upstream. Feedback signals were added at each computational grid point in the feedback domain. The ordinary simulation was performed for the following upstream velocity boundary conditions:

- (A) velocity profile with the measured Doppler velocity,
- (B) velocity profile with the measured Doppler velocity scaled by flow rate estimation,
- (C) parabolic velocity profile with flow rate estimation,
- (D) uniform velocity profile with flow rate estimation.

UMI simulation was also performed with the same boundary conditions. The feedback gain was set to 100. The downstream boundary condition of all cases was free flow, and the no-slip condition was set on the wall. The blood flow rate was estimated to minimize the summation of the absolute value of the error between the measured and computed Doppler velocities in the feedback domain by means of the golden section method. The accuracy of the calculation was evaluated by the error norm defined as follows:

$$e = \frac{1}{N} \sum_n |V_c - V_m| / V_{type}, \quad (4)$$

where V_{type} is typical Doppler velocity at the carotid artery.

3. Results and Discussion

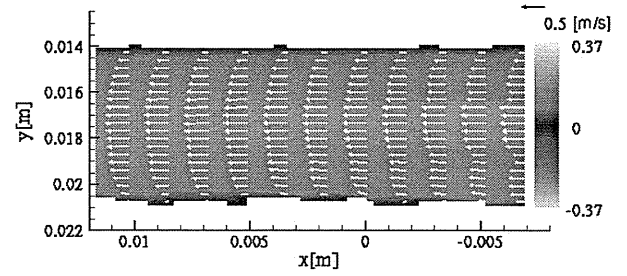
Figure 2 shows a comparison between the ordinary simulation and the UMI simulation for Case (B). In the result for the ordinary simulation in Fig. 2(a), the velocity profile converges to a parabolic distribution in the downstream direction. On the other hand, the result of the UMI simulation in Fig. 2(b) shows downstream drift.

Next, the accuracy of the ordinary simulation and that of the UMI simulation were compared using the error norm of Eq. (4). In Fig. 3(a) for the ordinary simulation, the error norm of Case A was larger than those of the other cases. This implies that ultrasonic measurement in one cross section has some error in evaluating the flow rate. Comparing Cases B, C and D, the error norm of Case B is smallest. Also, for the UMI simulation in Fig. 3(b), the error norm in Case A was the largest, showing that applying the correct flow rate is important. The error norms for Cases B, C, and D are almost the same, implying that the UMI simulation is insensitive to the upstream boundary velocity profile. Comparison of Figs. 3 (a) and (b) shows that the error of the UMI simulation is almost half that of the ordinary simulation, revealing that the UMI simulation has a better accuracy than that of the ordinary simulation with measured upstream velocity condition.

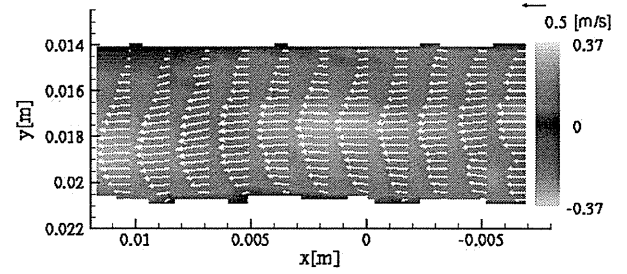
4. Concluding remarks

In this study, UMI simulation and ordinary simulation with several upstream velocity boundary conditions were performed for a blood flow in a carotid artery. The error of the UMI simulation was found to be almost half that of the ordinary simulation with measured upstream

velocity condition, showing a better accuracy in reproducing the blood flow.

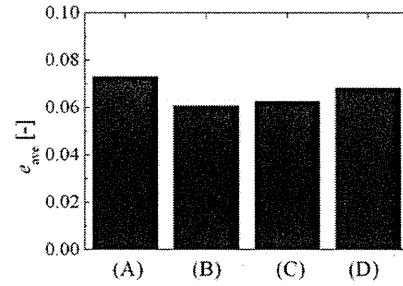


(a) Ordinary simulation.

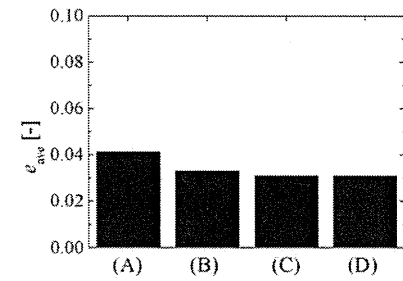


(b) UMI simulation

Fig. 2 Comparison of velocity fields for Case (B)



(a) Ordinary simulation.



(b) UMI simulation

Fig. 3 Comparison of error norm

References

- [1] Funamoto K, et al. Fundamental Study of Ultrasonic -Measurement-Integrated Simulation of Real Blood Flow in the Aorta. *Ann Biomed Eng* 33, 415-428, (2005).
- [2] Kato T, et al. Evaluation of Wall Shear Stress on Carotid Artery with Ultrasonic-Measurement-Integrated Simulation. *Seventh International Conference on Flow Dynamics*, 542-543, (2010).

Review Article

Evaluation of the Effects of Acupuncture on Blood Flow in Humans with Ultrasound Color Doppler Imaging

Shin Takayama,¹ Masashi Watanabe,¹ Hiroko Kusuyama,¹ Satoru Nagase,² Takashi Seki,¹ Toru Nakazawa,³ and Nobuo Yaegashi^{1,2}

¹ Department of Traditional Asian Medicine, Graduate School of Medicine, Tohoku University, 2-1, Seiryomachi, Aoba-ku, Sendai 980-8575, Japan

² Department of Obstetrics and Gynecology, Tohoku University Graduate School of Medicine, Sendai 980-8574, Japan

³ Department of Ophthalmology and Visual Science, Graduate School of Medicine, Tohoku University, Sendai 980-8575, Japan

Correspondence should be addressed to Shin Takayama, tatahara1492@gmail.com

Received 23 February 2012; Revised 2 April 2012; Accepted 2 April 2012

Academic Editor: Gerhard Litscher

Copyright © 2012 Shin Takayama et al. This is an open access article distributed under the Creative Commons Attribution License, which permits unrestricted use, distribution, and reproduction in any medium, provided the original work is properly cited.

Color Doppler imaging (CDI) can be used to noninvasively create images of human blood vessels and quantitatively evaluate blood flow in real-time. The purpose of this study was to assess the effects of acupuncture on the blood flow of the peripheral, mesenteric, and retrobulbar arteries by CDI. Statistical significance was defined as *P* values less than 0.05. Blood flow in the radial and brachial arteries was significantly lower during needle stimulation on LR3 than before in healthy volunteers, but was significantly higher after needle stimulation than before. LR3 stimulation also resulted in a significant decrease in the vascular resistance of the short posterior ciliary artery and no significant change of blood flow through the superior mesenteric artery (SMA) during acupuncture. In contrast, ST36 stimulation resulted in a significant increase in blood flow through the SMA and no significant change in the vascular resistance of the retrobulbar arteries. Additionally, acupuncture at previously determined acupoints in patients with open-angle glaucoma led to a significant reduction in the vascular resistance of the central retinal artery and short posterior ciliary artery. Our results suggest that acupuncture can affect blood flow of the peripheral, mesenteric, and retrobulbar arteries, and CDI can be useful to evaluate hemodynamic changes by acupuncture.

1. Introduction

To date, no quantitative evaluation methods have been established for determining the physiological effectiveness of acupuncture. Therefore, researchers conduct experiments using a variety of approaches. In this study, we focused on the physiological reactions to acupuncture and investigated blood flow changes that result from acupuncture [1–5].

Many studies of acupuncture efficacy have been based on the results of animal experiments with anesthesia. These studies indicate that acupuncture works through physiological mechanisms that occur primarily in the autonomic nervous system [6–12]. When acupuncture is performed in human clinical practice, the conditions are very different from those in animal experiments. Additionally, because the invasive examination techniques that are often used to evaluate the results of acupuncture treatments affect the

efficacy of those treatments, it is difficult to distinguish physiological reactions caused by acupuncture from those caused by the invasion necessary for examination. To determine the efficacy of acupuncture in humans, it is important that the examination method be noninvasive. We therefore used noninvasive color Doppler imaging (CDI) with ultrasound to evaluate blood flow. CDI is an examination technique that is widely used in the practice and research of Western medicine [13–21]. CDI can quantitatively measure intravascular blood flow in the extremities and in various organs in real-time. It is useful in the investigation of vessels, such as the peripheral, coronary, splenic, adrenal, and superior mesenteric arteries (SMA) [22]. In addition, the reproducibility of real-time and noninvasive hemodynamic measurement with CDI is reported elsewhere [23].

In traditional Chinese medicine, LR3 (Taichong, located on the foot, 1.5–2 units above the web between the

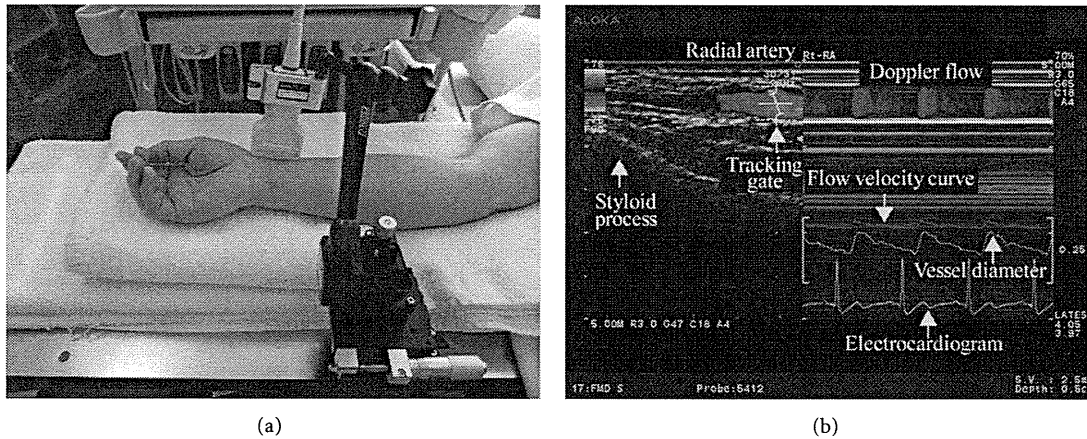


FIGURE 1: (a) Ultrasound measurement of the radial artery. 13 MHz linear transducer is fixed along radial artery with a special probe holder (MP-PH0001, Aloka Co., Ltd., Tokyo, Japan). (b) Display of CDI. Left: the vessel image and the position of the artery tracking gate. Right: changes in vessel diameter, Doppler flow, and flow velocity as determined by an automated edge-detection device and computer analysis software (e-Tracking system; Aloka Co., Ltd., Tokyo, Japan).

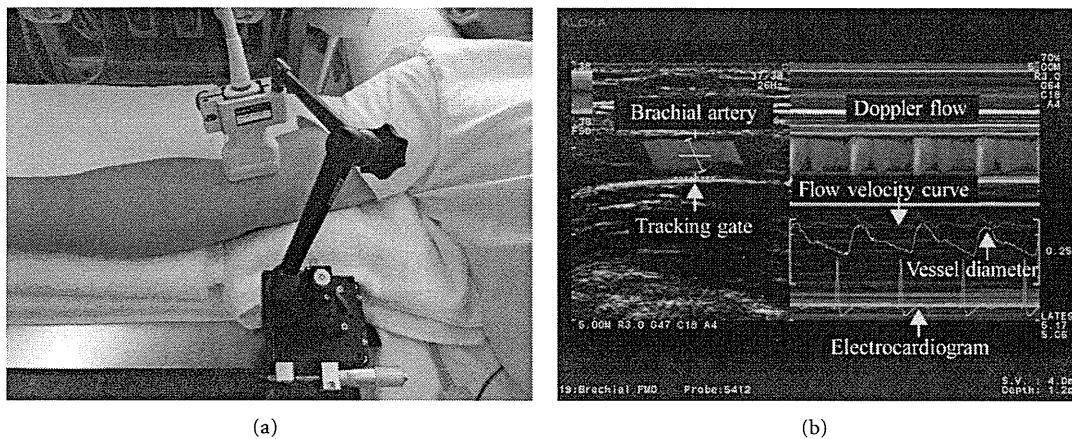


FIGURE 2: (a) Ultrasound measurement of the brachial artery. 13 MHz linear transducer is fixed along brachial artery with a special probe holder (MP-PH0001, Aloka Co., Ltd., Tokyo, Japan). (b) Display of CDI. Left: image of the vessel image and position of the artery tracking gate. Right: changes in vessel diameter, Doppler flow, and flow velocity, as determined by an automated edge detection device and computer analysis software (e-Tracking system; Aloka Co., Ltd., Tokyo, Japan).

first and second toes [24]) is an acupoint on the liver meridian, which has the functions of “soothing the liver,” “regulating the blood,” and “opening into the eyes” [24]. We therefore hypothesized that LR3 acupuncture would affect hemodynamics in the peripheral arteries and the retrobulbar arteries. ST36 (Zusanli, located on the lower leg, 3 units below the lateral “eye” of the knee, approximately 1 finger width lateral to the tibia [24]), in contrast, is an acupoint on the stomach meridian, and is associated with the functions of gastrointestinal organs [25]. We therefore hypothesized that ST36 acupuncture would affect hemodynamics in the SMA. Because glaucoma prognosis and retrobulbar circulation are related [26–29], we also investigated the effects of acupuncture on retrobulbar circulation in open-angle glaucoma (OAG) patients. In this study, we introduce the noninvasive CDI with ultrasound to evaluate blood flow changes by acupuncture.

2. Materials and Methods

2.1. Ultrasound Technique for Blood Flow Measurement. We measured circulation in the upper limb, SMA, and retrobulbar vessels using an ultrasound system (Prosound $\alpha 10$; Aloka Co., Ltd, Tokyo, Japan). The system had a 13 MHz linear transducer and a 5 MHz convex transducer. We used the linear transducer to examine peripheral arteries and the retrobulbar vessels. We used the convex transducer to measure SMA circulation.

The radial artery was examined just medial to the radial styloid process (Figure 1). The brachial artery was monitored immediately proximal to the elbow (Figure 2). The SMA supplies blood to the whole small intestine, except for the superior part of the duodenum. It also supplies blood to the cecum, the ascending colon, and most of the transverse colon. SMA measurements were acquired within 2–3 cm of

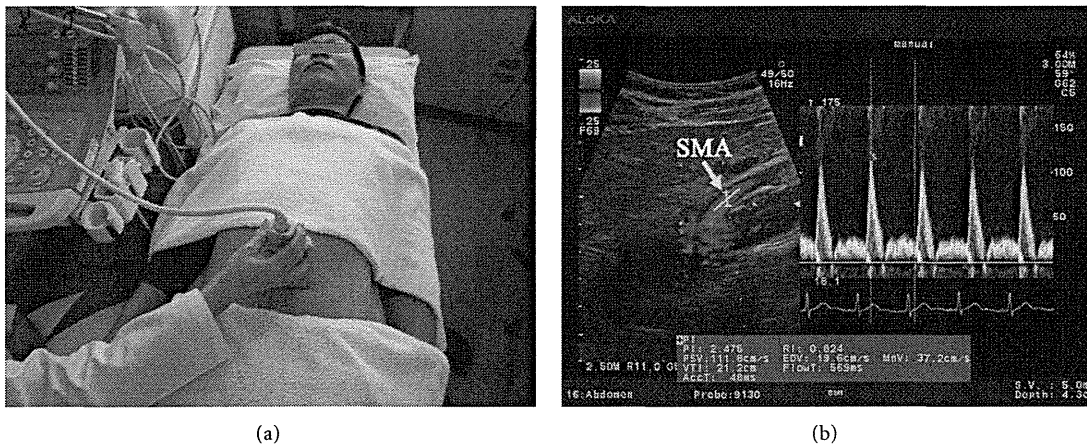


FIGURE 3: (a) Ultrasound measurement of the SMA. 5 MHz convex transducer is positioned on the abdomen. (b) Display of CDI. Left: image of the vessel and the position of the artery tracking. Right: Doppler flow and flow velocity.

the artery origin (Figure 3) [30, 31]. Avoiding any pressure on the eye, CDI was performed for the retrobulbar vessels, including the ophthalmic artery (OA), central retinal artery (CRA), and nasal or temporal short posterior ciliary artery (Figures 4 and 5). The OA was examined approximately 20 mm behind the globe (Figure 5(b)), the CRA was examined within 5 mm of the retrolaminar portion of the optic nerve (Figure 5(c)), and the nasal or temporal SPCA that obtained clear image was examined approximately 5–10 mm behind the globe (Figure 5(d)). Blood flow was monitored continuously [32, 33] and we employed a Doppler angle of 60° or less for each measurement [34, 35]. Each Doppler waveform was automatically drawn and calculated using the software included with the ultrasound system. The following calculations were used to determine the hemodynamic parameters at each site [30, 31].

- (i) Vessel diameter (VD).
- (ii) Cross-sectional area (CSA) = $(VD/2)^2 \times \pi$.
- (iii) Peak systolic velocity (PSV).
- (iv) End-diastolic velocity (EDV).
- (v) Resistive index (RI) = $(PSV - EDV)/PSV$.
- (vi) Mean flow velocity (MV).
- (vii) Blood flow volume = $CSA \times MV$.

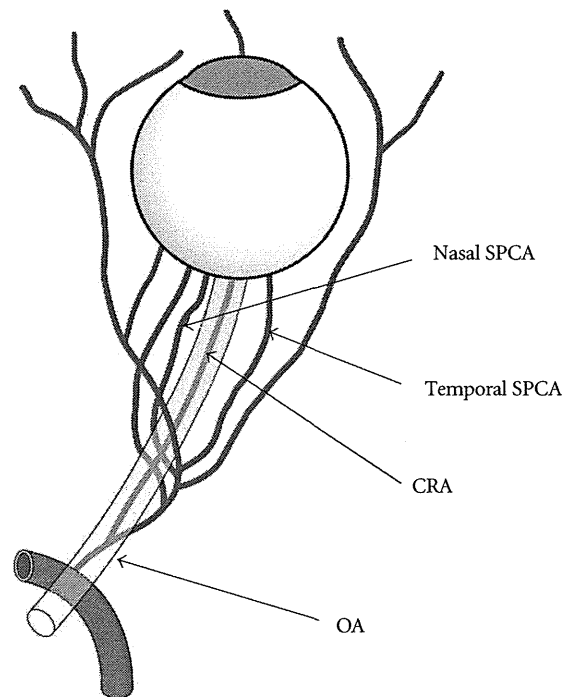


FIGURE 4: Schema of the retrobulbar arteries (OA: ophthalmic artery, CRA: central retinal artery, and SPCA: short posterior ciliary artery).

2.2. Statistical Analysis. Statistical analysis was performed with SPSS software (version 16.0, SPSS Japan Inc., Tokyo, Japan). Repeated measure analysis of variance, followed by Dunnett's post hoc test, was used for statistical comparison between the measure points. Comparison between rest and after acupuncture was done by paired *t*-test. Results are presented as the mean \pm SD and $P < 0.05$ was taken to indicate significance for all statistical analysis.

2.3. Experiment 1: Effects of LR3 Acupuncture on Upper Limb Circulation [1]. This study was employed to investigate the upper limb circulation after acupuncture at LR3 acupoints on foot. The participants were recruited by the

poster recruitment in Tohoku University. Eighteen healthy volunteers (mean age: 32 ± 5 years; 14 males and 4 females) were enrolled in this study. A disposable fine stainless-steel needle (diameter: 0.16 mm; length: 40 mm; Seirin Co., Ltd., Shizuoka, Japan) was inserted on LR3 bilaterally and maintained at a depth of 10 mm during the test. After the needle was inserted, stimulation (rotating the needles manually within an angle of 90 degrees) was performed for 18 seconds. The needles were removed 200 seconds after acupuncture. Radial and brachial CDI were performed before acupuncture; during acupuncture treatment; 30, 60, and 180 seconds after acupuncture.

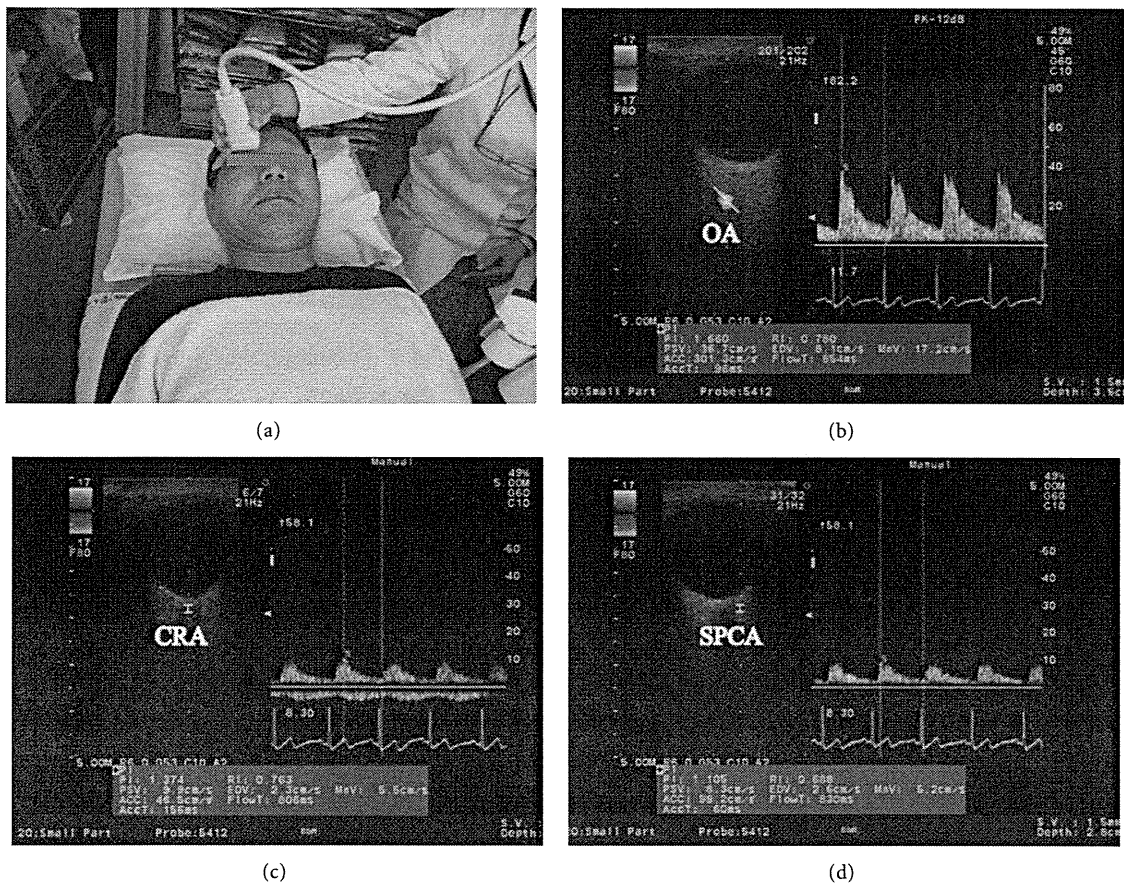


FIGURE 5: (a) Ultrasound measurement of retrobulbar arteries. 13 MHz linier transducer is attached on the eyelid. Horizontal scans by CDI through the ocular globe showing the (b) ophthalmic artery (OA), (c) central retinal artery (CRA), and (d) temporal short posterior ciliary artery (SPCA). Left: image of the vessel and the position of the artery tracking. Right: Doppler flow and flow velocity (b, c, and d).

2.4. Experiment 2: Effects of LR3 Acupuncture on Blood Circulation to the Eye and through the SMA. This study was employed to clarify the hemodynamic changes by acupuncture in two different organs (intestine and eye) with simultaneous evaluation by ultrasound. The participants were recruited by the poster recruitment in Tohoku University. Thirteen healthy volunteers (mean age: 36 ± 9 years; 10 males and 3 females) were enrolled in this study. Acupuncture was performed bilaterally on LR3 with manual needle rotation and the disposable stainless steel needles ($0.16 \text{ mm} \times 40 \text{ mm}$; Seirin Co. Ltd., Shizuoka, Japan) were kept at the same site for 15 minutes. Retrobulbar vessels and SMA circulation were measured simultaneously at rest and 15 minutes after the start of acupuncture using ultrasound.

2.5. Experiment 3: Effects of ST36 Acupuncture Blood Circulation to the Eye and through the SMA. This study was also employed to clarify the hemodynamic changes by acupuncture in two different organs (intestine and eye) with simultaneous evaluation by ultrasound. The participants were recruited by the poster recruitment in Tohoku University. Thirteen subjects (mean age: 36 ± 8 years; 10 males and 3 females) were enrolled in this study. Acupuncture was performed bilaterally on ST36 with manual rotation of the

disposable stainless steel needles ($0.16 \text{ mm} \times 40 \text{ mm}$; Seirin Co. Ltd., Shizuoka, Japan) were kept in the same site for 15 minutes. Retrobulbar vessels and SMA circulation were measured simultaneously at rest and 15 minutes after the start of acupuncture using ultrasound.

2.6. Experiment 4: Effects of Acupuncture on Retrobulbar Circulation in OAG Patients [2]. The relation between glaucoma and retrobulbar circulation in the prognosis of the disease has been indicated [26–29], therefore we investigated the effects of acupuncture on OAG patients by CDI. The patients were recruited in the outpatient clinic of ophthalmology in Tohoku University Hospital. Eleven OAG patients (mean age: 63 ± 11 years; 1 male and 10 females; 20 eyes with OAG) were enrolled. All patients included in the study had been treated with topical antiglaucoma medications for at least 3 months prior to the study. As a control, the subjects received the measurements of retrobulbar vessel hemodynamics that were performed at rest and one hour after the first measurement. One month later, they received the same measurements before and after acupuncture treatment. Acupuncture was performed once bilaterally at acupoints BL2, EX-HN5, ST2, ST36, SP6, KI3, LR3, GB20, BL18, and BL23 for 15 minutes using disposable stainless steel needles

TABLE 1: Hemodynamic parameters and blood flow volume of the radial and brachial arteries by acupuncture on LR3. The values represent the mean and SD. * $P < 0.05$, ** $P < 0.01$ versus before acupuncture. Modified from [1].

Parameters	Acupuncture on LR3				
	Before	During	30 s after	60 s after	180 s after
Systolic blood pressure (mmHg)	116.8 ± 10.1				114.5 ± 12.3
Diastolic blood pressure (mmHg)	67.3 ± 8.4				65.8 ± 7.3
Heart rate (beats/min)	67.3 ± 10.1	64.2 ± 8.8	65.8 ± 9.3	66.2 ± 9.3	66.9 ± 9.6
Blood flow volume of the radial artery (mL/min)	56.3 ± 33.5	25.4 ± 26.3	57.9 ± 47.5	67.7 ± 44.7	67.0 ± 36.5
Blood flow volume of the brachial artery (mL/min)	87.5 ± 56.4	65.7 ± 41.6	86.8 ± 53.7	90.1 ± 51.5	106.5 ± 59.8

TABLE 2: Hemodynamic parameters, blood flow volume of the SMA, and resistive index of retrobulbar arteries by acupuncture on LR3. The values represent the mean and SD. * $P < 0.05$, ** $P < 0.01$ versus before acupuncture.

Parameters	Acupuncture on LR3	
	Before	After
Systolic blood pressure (mmHg)	119.6 ± 12.8	116.7 ± 11.1
Diastolic blood pressure (mmHg)	77.7 ± 9.4	76.5 ± 9.3
Heart rate (beats/min)	66.8 ± 7.1	63.3 ± 4.6**
Blood flow volume of the SMA (mL/min)	734.8 ± 312.9	704.4 ± 328.1
RI in OA	0.719 ± 0.097	0.707 ± 0.089
RI in CRA	0.661 ± 0.088	0.644 ± 0.052
RI in SPCA	0.624 ± 0.057	0.580 ± 0.037*

(0.16 mm or 0.20 mm × 40 mm; Seirin Co. Ltd., Shizuoka, Japan). Retrobulbar circulation was measured using CDI at rest prior to treatment and 1 hour later, or after acupuncture.

3. Results and Discussion

3.1. Experiment 1: Effects of LR3 Acupuncture on Upper Limb Circulation [1]. Hemodynamic parameters including blood pressure, heart rate, and blood flow volume in the radial and brachial arteries are summarized in Table 1. Figure 6 illustrates the profile of the percent changes in blood flow volume in the radial and brachial arteries. The blood flow volume in the radial artery decreased significantly during acupuncture ($P < 0.01$), but showed a significant increase at 180 seconds after acupuncture ($P < 0.05$) (Figure 6). In the brachial artery, the blood flow volume also showed a significant increase at 180 seconds after acupuncture ($P < 0.05$) (Figure 6). The physiological mechanisms of decrease and increase blood flow volume in upper limb are presumably related to a peripheral vascular resistance due to an instantaneous increase and decrease in sympathetic tone [1]. The present result suggests that LR3 located on the foot and apart from the upper limb can affect the circulation in the upper limb.

3.2. Experiment 2: Effects of LR3 Acupuncture on Blood Circulation to the Eye and through the SMA. The RI of the SPCA was significantly lower after acupuncture than before ($P < 0.05$; Table 2). However, blood flow volume in the SMA was not significantly changed after acupuncture than before (Table 2). The SPCA is the ocular branches of the OA and it supplies blood to the choroid (Figure 4) [32]. The decrease of the distal vascular resistance in the SPCA that

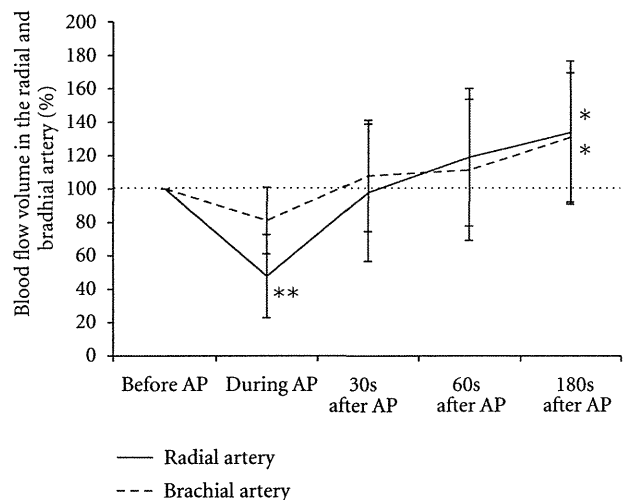


FIGURE 6: Percent changes in blood flow volume in the radial and brachial arteries before, during, and after acupuncture treatment. Values are presented as a percentage of the pretreatment blood flow. Values represent the mean and SD. AP: acupuncture. * $P < 0.05$, ** $P < 0.01$ versus before acupuncture. Modified from [1].

we observed indicates that acupuncture on LR3 results in an increase of the blood flow to the choroid. It has been reported that the blood flow in the eye is controlled by sympathetic and parasympathetic nerves, and it is related with the release of nitric oxide or calcitonin gene-related peptide [33, 34]; it has also been reported that the regulation of regional blood flow by somatic afferent stimulation is based on somatoautonomic reflex mechanisms in the choroidal blood flow of the eyeball [34]. The hemodynamic changes in the SPCA by acupuncture may be related with these